

Chemotaxis in uncertain environments: hedging bets with multiple receptors

Austin Hopkins¹ and Brian A. Camley²

¹Department of Physics & Astronomy, Johns Hopkins University

²Department of Physics & Astronomy, Department of Biophysics, Johns Hopkins University

Eukaryotic cells are able to sense chemical gradients over a wide range of different environments. We show that, if a cell is exposed to a widely variable environment, cells may gain additional chemotactic accuracy by expressing multiple types of receptors with varying affinities for the same signal. As the uncertainty of the environment is increased, there is a transition between cells preferring to express a single receptor type and a mixture of types – hedging their bets against the possibility of an unfavorable environment. We use this to predict the optimal receptor dissociation constants given a particular environment. In sensing this signal, cells may also integrate their measurement over time. Surprisingly, time-integration with multiple receptor types is qualitatively different from gradient sensing by a single receptor type – it is possible for cells to extract orders of magnitude more information out of a signal by using a maximum likelihood estimate than naive time integration.

As a white blood cell finds a wound, or an amoeba finds nutrition, they chemotax, sensing and following chemical gradients. Eukaryotic cells sense gradients of chemical ligands by measuring ligand binding to receptors on the cell's surface. In eukaryotic chemotaxis in shallow gradients, accuracy is often limited by the fundamental stochasticity in this signal arising from randomness in ligand-receptor binding and diffusion [1–4]. Eukaryotic chemotaxis has been extensively modeled [1, 5, 6], including extensions to collective chemotaxis [7–10], stochastic simulation [11, 12], and detailed mechanical and biochemical models [13, 14]. Both modeling and experiment find that eukaryotic chemotaxis is most accurate at ligand concentrations near the receptor's dissociation constant K_D [2, 3, 5]. Cells, in crawling through tissue and searching for targets at vastly varying concentrations, are naturally exposed to a huge variation in environmental signals. To what extent can cells gain chemotactic function in these different environments by expressing multiple different receptors with differing affinity for the ligand, or altering receptor affinity [4, 15–17] (see [4] for initial modeling)? If a cell is sufficiently uncertain about its chemical environment, the cell should express multiple receptors. We provide results for the optimal receptor K_{DS} depending on this uncertainty. In addition, we find that integrating information from multiple measurements of the receptor state is more complicated in the many-receptor case, and show that a standard approach significantly under-estimates the ability of a cell to sense gradients.

We generalize the model of [5, 18], considering a cell with receptors of R types with dissociation constants K_D^i , $i = 1 \dots R$, with each receptor type spread evenly over a circular cell. We find the fundamental limit set by the Cramér-Rao bound with which this cell can measure a shallow gradient g by using a snapshot of current receptor occupation. If the concentration near the cell is locally $c(\mathbf{r}) = c_0 e^{\mathbf{r} \cdot \mathbf{g}/L}$, i.e. g is the percentage change across the cell diameter L , this uncertainty is (Appendix)

$$\sigma_g^2 = \sigma_{g_x}^2 + \sigma_{g_y}^2 = \frac{16}{N \sum_{i=1}^R f_i \frac{c_0 K_D^i}{(c_0 + K_D^i)^2}} \quad (\text{snapshot}) \quad (1)$$

where N is the total number of receptors, and f_i is the fraction of those receptors that are of type i .

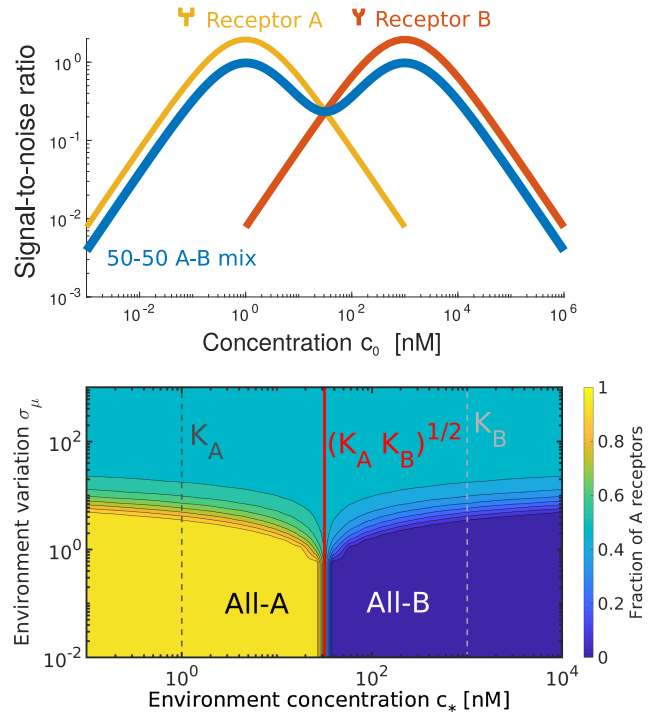


FIG. 1: Cells benefit from mixed receptor expression when their environment is uncertain— TOP: The signal-to-noise ratio g^2/σ_g^2 from Eq. 1 is plotted, showing the SNR from having 100% A receptors (yellow), 100% B receptors (red) or both in a 50-50 combination (blue). BOTTOM: Fraction of A receptors that maximizes CI for snapshot measurements (Eq. 1) as a function of $p(c_0)$ where $p(\ln c_0) \sim e^{-(\ln c_0 - \ln c_*)^2/2\sigma_\mu^2}$, characterized by the environment concentration c_* and the standard deviation of the log of the concentration, σ_μ . The transition between All- A and All- B occurs at $\sqrt{K_A K_B}$ at low uncertainty, as predicted. Dashed lines indicate receptor K_D . $K_A = 1$ nM, $K_B = 1000$ nM, $N = 5 \times 10^4$ and $g = 0.05$ are used in both plots.

When can a cell improve its accuracy by expressing multiple receptor types? If we try to maximize the signal-to-noise ratio $\text{SNR} = g^2/\sigma_g^2$, we see from Eq. 1 that SNR is a linear function of the f_i , and will be maximized by choosing $f = 1$ for the receptor type with the largest value of $\frac{c_0 K_D^i}{(c_0 + K_D^i)^2}$,

and $f = 0$ for the others. For the simplest case of two receptor types A and B with dissociation constants K_A, K_B ($K_B > K_A$) this means that the best accuracy occurs with all A receptors when $c_0 < \sqrt{K_A K_B}$, and with all B receptors when $c_0 > \sqrt{K_A K_B}$ (Fig. 1, top).

If the background concentration is completely known, it is never beneficial for a cell to express multiple receptor types simultaneously. However, if a cell is uncertain about the concentration it is likely to encounter, it may hedge its bets by choosing to express multiple receptor types, allowing it to effectively gradient sense in more environments. Does a cell in concentration c_0 with probability $p(c_0)$ benefit from multiple receptor types? What metric is appropriate? We could compute the average signal-to-noise ratio, $\text{SNR} = \int dc_0 p(c_0) g^2 / \sigma_g^2$. However, increasing SNR at one concentration is little consolation to the cell that finds itself completely lost at another concentration – the utility of SNR saturates. We therefore argue that a natural metric is the mean chemotactic index $\overline{\text{CI}}$, where $\text{CI} = f(\text{SNR})$, with $f(x)$ saturating at 1 as $x \rightarrow \infty$. Here, we use $f(x) = \sqrt{2x/\pi} L_{1/2}(-x/2)$, where $L_{1/2}(x)$ is a generalized Laguerre polynomial, as in [19]; however, alternate definitions of the chemotactic index lead to similar results.

In Fig. 1, we consider two receptors with dissociation constants K_A and K_B , and numerically determine the fraction of A receptors that maximizes $\overline{\text{CI}}$. We choose $p(c_0)$ to be log-normal, $p(\ln c_0) \sim e^{-(\ln c_0 - \ln c_*)^2/2\sigma_\mu^2}$ – a generic option when we expect large variability. When the environmental uncertainty σ_μ is small, we see the behavior predicted above – at small c_* , the cell should express all A receptors, while for $c_* > \sqrt{K_A K_B}$ the cell should switch to all-B. However, at larger uncertainty, cells optimize $\overline{\text{CI}}$ by expressing equal amounts of A and B receptors.

Why is a 50-50 mix optimal even when $c_* \approx K_A$? CI is only nonzero when c_0 is close to K_A or K_B (very roughly, $c_0 \sim \sqrt{K_A K_B}$). As σ_μ increases and $p(c_0)$ becomes more slowly-varying, the integral $\overline{\text{CI}} = \int dc_0 p(c_0) \text{CI}(c_0) \approx p(\sqrt{K_A K_B}) \int dc_0 \text{CI}(c_0)$. In this limit, while $\overline{\text{CI}}$ depends on c_* , the optimal fraction does not.

Our results in Fig. 1 explain when a cell should choose to mix a combination of receptor types or receptor states. Can we also find a unique solution for the receptors a cell would evolve to maximize gradient-sensing ability in a given $p(c_0)$? We optimize $\overline{\text{CI}}$ by varying K_D^i and receptor fraction f_i for different numbers of receptor types R and different widths σ_μ , holding the total number of receptors N constant. We choose the receptor configuration that maximizes $\overline{\text{CI}}$ – with an important caveat. By adding more receptor types with arbitrary K_D , we can always at least match the performance of a single receptor. We thus choose the configuration that maximizes $\overline{\text{CI}}$, but if many configurations generate roughly the same $\overline{\text{CI}}$ (within 0.01), we choose the one with the smallest number of receptor types R . In order to reduce the number of variables we optimize over, we use the symmetry of $p(c_0)$, assuming $\ln K_D^i$ and f_i are mirror-symmetric around $\ln c^*$. The resulting optimal K_D^i are shown in Fig. 2.

Fig. 1 and Fig. 2 are based on Eq. 1, which describes the

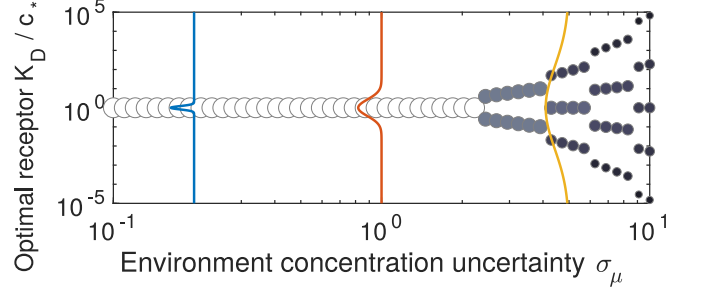


FIG. 2: **Optimal receptor configuration.** We show the types and K_D^i values for receptors as the environmental uncertainty σ_μ is increased. Marker areas are scaled to the optimal fraction of that receptor type. Solid lines plot $p(c_0)$. We choose $c_* = 1 \text{ nM}$, $N = 5 \times 10^4$ and $g = 0.05$, and choose the receptor configuration with the lowest number of types that is within 0.01 of the maximum $\overline{\text{CI}}$.

fundamental uncertainty with which a cell can sense a gradient *from a single snapshot of its receptor state*. If cells integrate their measurements over time, they can improve gradient sensing. Our results (Appendix) give the maximum likelihood estimator $\hat{\mathbf{g}}$ for the gradient vector \mathbf{g} given the snapshot data. Defining a time-integrated estimator $\hat{\mathbf{g}}_T = \frac{1}{T} \int_0^T \hat{\mathbf{g}}(t) dt$, as in earlier work [5, 8, 18], we find its variance, $\sigma_{g,T}^2 = \langle |\mathbf{g}_T - \mathbf{g}|^2 \rangle$. To do this, we must consider the kinetics of binding and unbinding at each receptor, which happens with a receptor correlation time of $\tau_i = 1/(k_+^i + c_0 k_-^i)$. In the limit of large averaging times $T \gg \tau_i$, we find (Appendix)

$$\sigma_{g,T}^2 = \frac{32 \sum_i^R f_i \beta_i \tau_i}{NT \left(\sum_i^R f_i \beta_i \right)^2} \quad (\text{naive average}) \quad (2)$$

where $\beta_i = c_0 K_D^i / (c_0 + K_D^i)^2$ reflects the accuracy of measuring only using receptor i – maximized at $c_0 = K_D^i$. For a single receptor, the gradient error is reduced by the effective number of measurements $2\tau_i/T$, $\sigma_{g,T}^2 = \sigma_g^2 \times 2\tau_i/T$ [5, 18]. Eq. 2 can be cast in a similar form as

$$\sigma_{g,T}^2 = \sigma_g^2 \sum_i^R \alpha_i \frac{2\tau_i}{T}$$

where $\alpha_i = \beta_i f_i / \sum_i^R \beta_i f_i$ is the weight given to receptor type i . This equation shows that the variance – in a naive time average – is reduced by a weighted sum that depends on the correlation times of the receptors. In the single receptor type case, $\sigma_{g,T}^2$ can become arbitrarily small as $\tau \rightarrow 0$. However, because the variance is proportional to the a weighted sum of τ_i/T , when receptor correlation times τ_i decrease, the error is limited by the slowest correlation time. If one receptor's correlation time is significantly faster than the other's, Eq. 2 predicts that you could reduce error merely by removing the slow receptors. The naive time average, therefore, does not efficiently use the information available.

This situation is reminiscent of a well-known result for concentration sensing: it is not optimal for a single receptor to

estimate c by computing a simple time-average of its occupation, $T^{-1} \int_0^T n(t)dt$. When, instead, the whole history of binding and unbinding events is used in a maximum likelihood estimate, the error σ_c^2 is reduced by two [20]. We therefore generalize the maximum likelihood results of [20] to determine the uncertainty of gradient sensing using the entire receptor trajectory (Appendix), finding (again in the limit $T \gg \tau_i$):

$$\sigma_{g,T;MLE}^2 = \frac{16}{N \sum_i^R f_i \beta_i \frac{T}{\tau_i}} \quad (\text{maximum likelihood}) \quad (3)$$

or more intuitively,

$$\sigma_{g,T;MLE}^2 = \sigma_g^2 \frac{1}{\sum_i^R \alpha_i \frac{T}{\tau_i}}$$

For a single receptor type, Eq. 3 is a factor of two smaller than the naive time average Eq. 2, precisely as in concentration sensing. However, for multiple receptors, the maximum likelihood time average can be orders of magnitude better, as the time correlation factors τ_i/T add “in parallel” – error is no longer limited by the slowest receptor.

We illustrate the differences between these two errors in Fig. 3, computing the SNR g^2/σ_g^2 for a system of two receptor types. Which type provides more information depends on the relative off rates of the two types:

$$\text{SNR}_{MLE} = \frac{Ng^2 k_-^A T}{16} \left[f_A \frac{c_0}{c_0 + K_A} + (1 - f_A) \rho \frac{c_0}{c_0 + K_B} \right] \quad (4)$$

where $\rho = k_-^B/k_-^A$.

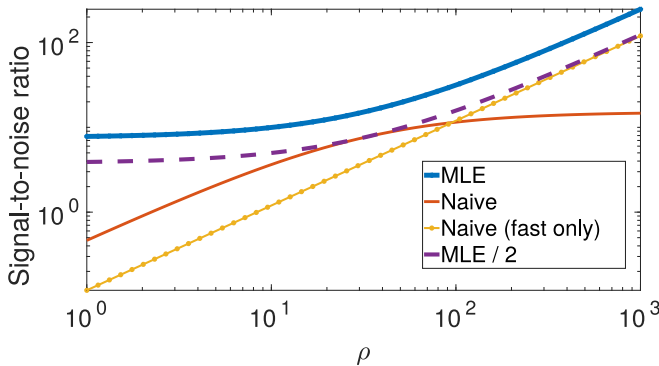


FIG. 3: Maximum likelihood estimate of gradient is much more accurate than naive averaging.— The SNR g^2/σ_g^2 is plotted as a function of $\rho = k_-^B/k_-^A$; $\rho > 1$ corresponds to the limit where B receptors have faster off rates. SNR is much larger using the MLE method; even in the best case, the naive average only reaches half of the MLE SNR. This is illustrated with a two-receptor system, $N = 5 \times 10^4$, $g = 0.05$, and we choose $K_A = 1 \text{ nM}$, $K_B = 1000 \text{ nM}$, with a fixed concentration $c_0 = \sqrt{K_A K_B}$ and $f_A = 0.5$, with $k_-^A T = 2$.

We see in Fig. 3 that as ρ is varied, the naive time average is always *at least* a factor of two lower in SNR than the MLE

result. In the limit where the B receptor off rate is large ($\rho \gg 1$), the naive average is worse than if only the $N/2$ B receptors were used. In this limit, the majority of the information is coming from the B receptors, and using only the B receptors reaches half the MLE SNR (Fig. 3).

How does time averaging affect bet-hedging? For a single environmental concentration, all- A is optimal when Eq. 4 increases with increasing f_A , i.e. $c_0/(c_0 + K_A) > \rho c_0/(c_0 + K_B)$, or $c_0 < c_{bal} \equiv \frac{K_B - K_A \rho}{\rho - 1}$. We see then that for $\rho = 1$, it is always best to use the lower- K_D receptor. The trade-offs are more complex when B receptors are faster. The balancing point c_{bal} varies from $c_{bal} \rightarrow \infty$ at $\rho = 1$ to $c_{bal} = 0$ at $\rho = K_B/K_A$. The point $\rho = K_B/K_A$ corresponds to the condition where the on rates of the two receptors are equal, $k_+^A = k_+^B$, as $k_-^B/k_-^A = K_B/K_A = \frac{k_-^B}{k_-^A} \frac{k_+^A}{k_+^B}$ – this would be the case if the on rates were diffusion-limited.

This crucial dependence on the off rates of the two receptors is preserved when we study the optimal configuration of receptors in an uncertain environment. In Fig. 4, we show how the optimal share of A receptors depends on the ratio of the off rates $\rho = k_-^B/k_-^A$. Even in the presence of significant uncertainty, when $\rho = 1$, all- A is optimal. However, at higher values of ρ , we find that the transition between all- A and all- B observed in Fig. 1 is preserved, occurring when the environmental concentration $c_* = c_{bal}$ (white dashed line). By contrast with the snapshot results, we see that at large uncertainties $\sigma_\mu > 1$, for $\rho = 10, 100$ we do not see a transition to a 50-50 mixture of receptors being optimal. Instead, at high uncertainties, the optimal receptor fraction becomes similar above and below c_{bal} , and the fraction of A receptors exceeds 0.5, with f_A then decreasing at even higher uncertainties ($\sigma_\mu > 10$). Why? When receptors time-average, CI can be nonzero over a broad range of c_0 (see Fig. 4, top), we see that our argument for the snapshot case fails, and it is not surprising that the optimal fraction varies with environmental concentration. We also caution that at these large levels of environmental variation, the difference between the optimal receptor configuration and simply choosing all- A or all- B receptors is small (Appendix) – at sufficiently high uncertainties, no configuration is particularly successful.

Can we produce a plot such as Fig. 2 showing the optimal receptor configuration if time-averaging is performed? When time averaging, error will be minimized by making the correlation times as small as possible – i.e. by taking $k_- \rightarrow \infty$. There does not appear to be a consistent way to argue a particular set of receptors is optimal unless k_- is restricted by some physical limit. This is because, as recognized for concentration sensing [20], only receptor binding rates are sensitive to c – bound times should be minimized. If we are in the limit of measurement times much longer than correlation times (Eq. 3), the optimal receptor off rates are set more by biochemical constraints than our accuracy limits.

Discussion.— Cells can express receptors with broadly variable K_D values, which can vary depending on receptor modification. For instance, kinetic measurements suggest that Dictyostelium has receptors for folic acid with K_D values ranging from 2 nM to 450 nM [17]. Receptors for cAMP

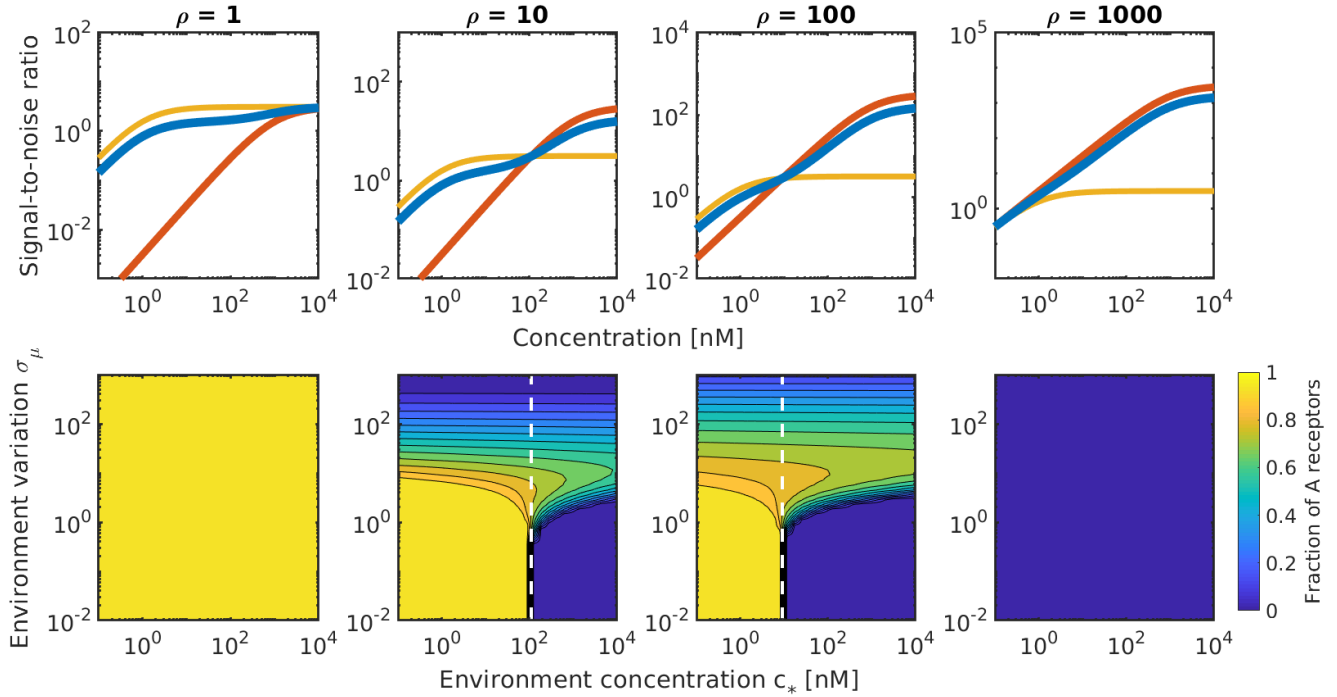


FIG. 4: **Tradeoff between two receptor types depends on their dynamic properties**—. TOP: SNR calculated for differing values of ρ at different fixed concentrations c_0 using Eq. 4. As in Fig. 1, yellow indicates all- A , red all- B and blue a 50-50 mix. BOTTOM: Optimal receptor fraction with time-averaging. Dashed white lines show the analytical c_{bal} . Parameters are as in Fig. 1 except $N = 10^4$ (chosen as cells have larger SNR with fewer receptors when time-averaging) and the length of time averaging is set to be $k^A T = 2$.

also have low and high affinity ranging over around a factor of 100 [21]. This includes both different receptor types and modifications of receptors that alter their affinity for ligand, e.g. phosphorylation or the binding of a G protein [15, 22]. Our results show that cells can hedge their bets against an uncertain environment by expressing multiple receptor types – but that this behavior is only reasonable if the uncertainty in c_0 spans the range of observed K_D (Fig. 2) – i.e. if cells are typically exploring environments where the uncertainty varies over orders of magnitude. (The idea that signal-processing should be adapted to the likely range of concentrations seen is similar to classical results showing that information transmission can be maximized by tuning input-output relationships to the input probability distribution [23].) In the case of chemotaxis to hunt bacteria, it seems intuitively plausible that observed concentrations span orders of magnitude, as bacterial hunting must function over both sparse and concentrated solutions, and over many distances to bacteria. However, we emphasize that at any fixed concentration, expressing multiple receptors is always suboptimal to adapting your receptors to the environment – so hedging is plausible in circumstances when the environment is uncertain *over the timescale on which the receptor affinity is fixed*. Our work thus suggests interesting future directions for extension, based on recent studies of concentration sensing in time-varying environments [24]. When

cells must express new receptors in order to alter their affinity, hedging is much more plausible than when faster receptor modification allows K_D to be changed. Future work could also consider multiple ligand types, which could also play a role in limiting accuracy by competing for receptors [25, 26]. It is not obvious how to design a reaction network that will reach the lower bound of Eq. 3, though it may be possible to extend recent work demonstrating routes to compute the maximum likelihood estimate involved in concentration sensing [26, 27]. One important difference here is that in order to find the maximum likelihood estimate \hat{g} , it is necessary to not just measure the bound and unbound times of each receptor, but to do this in a spatially resolved way that is distinct for each receptor type. In addition, we note that computation of the time-dependent maximum likelihood estimate for concentration requires additional free energy expenditure [27] – it would be interesting to determine if the extravagant benefits of the MLE approach for gradient sensing with multiple receptors (Fig. 3) comes with a commensurate cost. We argue that, though these are significant complexities, the huge gap between the fundamental bound of Eq. 3 and the naive average of Eq. 2 suggests that even very rough approximations to the MLE would provide significant gains over a naive average.

Acknowledgments. We thank Wouter-Jan Rappel and Emiliano Perez Ipiña for a close reading of the paper.

- [1] H. Levine and W.-J. Rappel, *Physics Today* **66** (2013).
- [2] D. Fuller, W. Chen, M. Adler, A. Groisman, H. Levine, W.-J. Rappel, and W. F. Loomis, *Proceedings of the National Academy of Sciences* **107**, 9656 (2010).
- [3] M. Ueda and T. Shibata, *Biophysical Journal* **93**, 11 (2007).
- [4] I. Segota, S. Mong, E. Neidich, A. Rachakonda, C. J. Lussenhop, and C. Franck, *Journal of The Royal Society Interface* **10**, 20130606 (2013).
- [5] B. Hu, W. Chen, W.-J. Rappel, and H. Levine, *Physical Review Letters* **105**, 048104 (2010).
- [6] R. G. Endres and N. S. Wingreen, *Proceedings of the National Academy of Sciences* **105**, 15749 (2008).
- [7] B. A. Camley, *Journal of Physics: Condensed Matter* **30**, 223001 (2018).
- [8] B. A. Camley and W.-J. Rappel, *Proceedings of the National Academy of Sciences* **114**, E10074 (2017).
- [9] A. Mugler, A. Levchenko, and I. Nemenman, *Proceedings of the National Academy of Sciences* p. 201509597 (2016).
- [10] A. Hopkins and B. A. Camley, *Physical Review E* **100**, 032417 (2019).
- [11] R. Sharma and E. Roberts, *Physical Biology* **13**, 036003 (2016).
- [12] V. Lakhani and T. C. Elston, *PLoS computational biology* **13**, e1005386 (2017).
- [13] C. Shi, C.-H. Huang, P. N. Devreotes, and P. A. Iglesias, *PLoS computational biology* **9**, e1003122 (2013).
- [14] I. Hecht, M. L. Skoge, P. G. Charest, E. Ben-Jacob, R. A. Firtel, W. F. Loomis, H. Levine, and W.-J. Rappel, *PLoS Computational Biology* **7** (2011).
- [15] Z. Xiao, Y. Yao, Y. Long, and P. Devreotes, *Journal of Biological Chemistry* **274**, 1440 (1999).
- [16] Y. Miyanaga, Y. Kamimura, H. Kuwayama, P. N. Devreotes, and M. Ueda, *Biochemical and Biophysical Research Communications* **507**, 304 (2018).
- [17] R. W. de Wit and P. J. van Haastert, *Biochimica et Biophysica Acta (BBA)-Biomembranes* **814**, 199 (1985).
- [18] B. Hu, W. Chen, W.-J. Rappel, and H. Levine, *Physical Review E* **83**, 021917 (2011).
- [19] B. A. Camley, J. Zimmermann, H. Levine, and W.-J. Rappel, *Physical Review Letters* **116**, 098101 (2016).
- [20] R. G. Endres and N. S. Wingreen, *Physical Review Letters* **103**, 158101 (2009).
- [21] R. L. Johnson, P. Van Haastert, A. R. Kimmel, C. L. Saxe, B. Jastorff, and P. N. Devreotes, *Journal of Biological Chemistry* **267**, 4600 (1992).
- [22] A. T. Islam, H. Yue, M. Scavello, P. Haldeman, W.-J. Rappel, and P. G. Charest, *Cellular signalling* **48**, 25 (2018).
- [23] W. Bialek, *Biophysics: searching for principles* (Princeton University Press, 2012).
- [24] T. Mora and I. Nemenman, *Physical Review Letters* **123**, 198101 (2019).
- [25] T. Mora, *Physical Review Letters* **115**, 038102 (2015).
- [26] V. Singh and I. Nemenman, *Physical Review Letters* **124**, 028101 (2020).
- [27] A. H. Lang, C. K. Fisher, T. Mora, and P. Mehta, *Physical Review Letters* **113**, 148103 (2014).
- [28] K. Wang, W.-J. Rappel, R. Kerr, and H. Levine, *Physical Review E* **75**, 061905 (2007).
- [29] K. Kaizu, W. de Ronde, J. Paijmans, K. Takahashi, F. Tostevin, and P. R. ten Wolde, *Biophysical Journal* **106**, 976 (2014).
- [30] W. Bialek and S. Setayeshgar, *Proceedings of the National Academy of Sciences of the United States of America* **102**, 10040 (2005).
- [31] A. M. Berezhkovskii and A. Szabo, *The Journal of Chemical Physics* **139**, 121910 (2013).

Supplementary Appendix for “Chemotaxis in Uncertain Environments”

Appendix A: Numerical details for minimization

In numerically maximizing $\overline{\text{CI}}$ as a function of the fractions of different receptors, we choose the Nelder-Mead method (Matlab’s fminsearch). We compute $\overline{\text{CI}}$ with adaptive Gauss-Kronrod quadrature (quadgk). In applying standard quadrature to this problem, it is important to be careful about the typical range over which the integrand $\text{CI}(c_0)p(c_0)$ is nonzero – depending on the parameters, this could be only near the K_D values for each receptor or more broad. We set fixed waypoints for the integral over all plausible ranges for the integrand to be nonzero, allowing this integral to be taken robustly.

Appendix B: Notation

This appendix includes calculations where we have to distinguish the type i and the index n of each receptor. The intermediate calculations are more complex than the final results in the main paper, and to help keep the details straight, we will denote receptor types i with superscripts and receptor indices n with subscripts. A superscript to a power i like C_n^i never denotes exponentiation. To keep consistent with this, we’ve included formulas with β^i where in the main text we’ve written β_i .

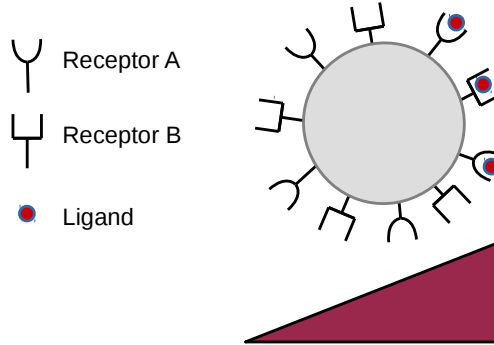


FIG. 5: Illustration of data used for gradient estimate using a snapshot of receptor state; only two receptor types are illustrated.

Appendix C: Snapshot sensing

How precisely can a cell make a measurement of a chemical gradient – using only its current information about which receptors on its surface are occupied? We extend results from [5, 18] on this accuracy to include multiple receptor types. We assume that the cell is in a shallow exponential gradient with direction ϕ and steepness $g = \frac{|\nabla C|}{C_0 L}$, where L is the diameter of the cell. The gradient \mathbf{g} can also be written as $\mathbf{g} = (g_x, g_y) = (g\cos(\phi), g\sin(\phi))$. The concentration at a cell receptor with angular coordinate φ can then be written as

$$C(\phi) = C_0 \exp \left[\frac{g}{2} \cos(\varphi - \phi) \right]. \quad (\text{C1})$$

Let there be R receptor types, where there are N^i receptors of type i and $N = \sum_i^R N^i$ total receptors. We describe the receptors as being uniformly spread across the cell, with angular positions φ_n^i (Fig. 5). Then each receptor of type i can be represented as a Bernoulli trial x_n^i with a probability of being occupied

$$P_n^i = C_n^i / (C_n^i + K_D^i), \quad (\text{C2})$$

where C_n^i is the concentration at the n th receptor of type i and K_D^i is the dissociation constant of receptor type i . The dissociation constant K_D^i is the ratio of unbinding and binding rates of the receptors of type i , i.e. $K_D^i = \frac{k_-^i}{k_+^i}$. Assuming that all the receptors

are independent of one another, we have the following likelihood function giving the probability of seeing receptor occupations x_i^n given gradient \mathbf{g}

$$\mathcal{L}(\mathbf{g}|x_1^0, \dots, x_{N^R}^R) = \prod_i^R \prod_n^{N^i} \left[(P_n^i)^{x_n^i} (1 - P_n^i)^{1-x_n^i} \right]. \quad (\text{C3})$$

The log-likelihood function is

$$\ln \mathcal{L} = \sum_i^R \sum_n^{N^i} \left[x_n^i \ln \left(\frac{C_n^i}{C_n^i + K_D^i} \right) + (1 - x_n^i) \ln \left(\frac{K_D^i}{C_n^i + K_D^i} \right) \right] \quad (\text{C4})$$

$$= \sum_i^R \sum_n^{N^i} \left[x_n^i \ln \left(\frac{C_n^i}{K_D^i} \right) + \ln \left(\frac{K_D^i}{C_n^i + K_D^i} \right) \right] \quad (\text{C5})$$

For the second term in this equation, we assume that the receptors are numerous enough that we can replace the sum over receptor position by a continuous integral, $\sum_n^{N^i} \rightarrow \frac{N^i}{2\pi} \int_0^{2\pi} d\varphi$:

$$\ln \mathcal{L} = \sum_i^R \left\{ \sum_n^{N^i} \left[\frac{1}{2} x_n^i g \cos(\varphi_n^i - \phi) + \ln \left(\frac{C_0}{K_D} \right) x_n^i \right] + \int_0^{2\pi} \frac{N^i}{2\pi} \ln \left(\frac{K_D^i}{C_0 \exp(\frac{g}{2} \cos(\varphi - \phi)) + K_D^i} \right) d\varphi \right\}. \quad (\text{C6})$$

We define $z_1^i = \sum_n^{N^i} x_n^i \cos \varphi_n^i$ and $z_2^i = \sum_n^{N^i} x_n^i \sin \varphi_n^i$, which measure the spatial asymmetry in the occupancy of receptors of type i . $Z_1 = \sum_i z_1^i$ and $Z_2 = \sum_i z_2^i$ measure the total spatial asymmetry in receptor occupancy of the cell. In a shallow exponential gradient, we can neglect terms $O(g^4)$ and higher for an estimation of the gradient $\vec{g} = (g_x, g_y)$. Then, the log-likelihood function becomes

$$\ln \mathcal{L} = \sum_i^R \left[\frac{g_x z_1^i + g_y z_2^i}{2} + \ln \frac{C_0}{K_D^i} \sum_n^{N^i} x_n^i - \frac{NC_0 f^i K_D^i (g_x^2 + g_y^2)}{16(C_0 + K_D^i)^2} + \ln \frac{C_0}{C_0 + K_D^i} \right]. \quad (\text{C7})$$

(We note that past papers with similar derivations [10, 18] have not always written the last term in this log-likelihood, which is an irrelevant constant.) Taking the derivative with respect to $g_{x,y}$ gives

$$\frac{\partial}{\partial g_{x,y}} \ln \mathcal{L} = \sum_i^R \left[\frac{z_{1,2}^i}{2} - \frac{NC_0 f^i K_D^i g_{x,y}}{8(C_0 + K_D^i)^2} \right] \quad (\text{C8})$$

Because the log function is monotonic, we can set Eq. C8 equal to zero to find \hat{g}_x and \hat{g}_y , the parameters which for g_x and g_y which maximize the likelihood function. Carrying out this procedure, we find:

$$\sum_i^R \left[\frac{z_{1,2}^i}{2} - \frac{NC_0 f^i K_D^i}{8(C_0 + K_D^i)^2} \hat{g}_{x,y} \right] = 0 \quad (\text{C9})$$

$$\sum_i^R \frac{z_{1,2}^i}{2} = \sum_i^R \left[\frac{NC_0 f^i K_D^i}{8(C_0 + K_D^i)^2} \hat{g}_{x,y} \right] \quad (\text{C10})$$

$$\frac{Z_{1,2}}{2} = \frac{NC_0}{8} \sum_i^R \left[\frac{f^i K_D^i}{(C_0 + K_D^i)^2} \hat{g}_{x,y} \right], \quad (\text{C11})$$

which be solved for $\hat{g}_{x,y}$ to determine estimators $\hat{g}_{x,y}$ as

$$\hat{g}_x = \frac{4Z_1}{NC_0 \sum_i^R \left[\frac{f^i K_D^i}{(C_0 + K_D^i)^2} \right]} \text{ and } \hat{g}_y = \frac{4Z_2}{NC_0 \sum_i^R \left[\frac{f^i K_D^i}{(C_0 + K_D^i)^2} \right]}. \quad (\text{C12})$$

To determine the asymptotic variance on these estimators, we will need to compute the second derivative of the log-likelihood function. Applying an additional derivative to Eq. C8 gives

$$\frac{\partial^2}{\partial g_{x,y}^2} \ln \mathcal{L} = -\frac{NC_0}{8} \sum_i^R \left[\frac{f^i K_D^i}{(C_0 + K_D^i)^2} \right]; \quad \frac{\partial^2}{\partial g_x \partial g_y} \ln \mathcal{L} = 0 \quad (\text{C13})$$

From the log-likelihood function, we can also determine the Fisher information matrix. In this case it is diagonal, and its inverse gives the variances of \hat{g}_x and \hat{g}_y in the limit of many samples. As a result, we have expressions for the asymptotic variances for \hat{g}_x and \hat{g}_y

$$\frac{1}{\sigma_{g_{x,y}}^2} = \left\langle \left(\frac{\partial \ln \mathcal{L}}{\partial g_{x,y}} \right)^2 \right\rangle = -\left\langle \frac{\partial^2 \ln \mathcal{L}}{\partial g_{x,y}^2} \right\rangle = \frac{NC_0}{8} \sum_i^R \left[\frac{f^i K_D^i}{(C_0 + K_D^i)^2} \right] \implies \sigma_{g_{x,y}}^2 = \frac{8}{NC_0 \sum_i^R \frac{f^i K_D^i}{(C_0 + K_D^i)^2}}. \quad (\text{C14})$$

The important parameter is $\sigma_{\mathbf{g}}^2$, which is just the sum of the component variances

$$\sigma_{\mathbf{g}}^2 = \sigma_{g_x}^2 + \sigma_{g_y}^2 = \frac{16}{NC_0 \sum_i^R \frac{f^i K_D^i}{(C_0 + K_D^i)^2}}. \quad (\text{C15})$$

As the sample size becomes large, the distribution of $\hat{g}_{1,2}$ converges to a normal distribution with means $g_{x,y}$ and variance $\sigma_{g_{x,y}}^2$. This also implies that the mean values of Z_1 and Z_2 are

$$\langle Z_{1,2} \rangle = \frac{1}{4} NC_0 \sum_i^R \left[\frac{f^i K_D^i}{(C_0 + K_D^i)^2} \right] g_{x,y}. \quad (\text{C16})$$

Appendix D: Naive time averaging

A cell may improve its estimation of the gradient by time averaging. In the previous section, we determined an estimator $\hat{\mathbf{g}}$ that is the best estimate of a cell's gradient, given a snapshot of its receptor information. Naively, a cell could improve its accuracy by making a measurement over a time T and determining the average of these estimates

$$\hat{\mathbf{g}}_T = \frac{1}{T} \int_0^T dt \hat{\mathbf{g}}(t) \quad (\text{D1})$$

Then the variance of this new estimator will be reduced,

$$\sigma_{g,T}^2 = \langle |\hat{\mathbf{g}}_T|^2 \rangle - \langle \hat{\mathbf{g}}_T \rangle^2 = \frac{1}{T^2} \int_0^T dt \int_0^T ds \left(\langle \hat{\mathbf{g}}(s) \hat{\mathbf{g}}(t) \rangle - \langle \hat{\mathbf{g}} \rangle^2 \right). \quad (\text{D2})$$

To understand how time averaging improves the cell's sensing accuracy, we need to compute $\langle \hat{\mathbf{g}}(s) \cdot \hat{\mathbf{g}}(t) \rangle$, the correlation function of $\hat{\mathbf{g}}$. This correlation function is related to the correlation functions in the estimates of each component of the gradient as

$$\langle \hat{\mathbf{g}}(s) \cdot \hat{\mathbf{g}}(t) \rangle = \langle \hat{g}_x(s) \hat{g}_x(t) \rangle + \langle \hat{g}_y(s) \hat{g}_y(t) \rangle. \quad (\text{D3})$$

And, by Eq. C12, the correlation functions for $g_{x,y}$ can be related to the correlation functions for $Z_{1,2}$ as

$$\langle \hat{g}_{x,y}(s) \hat{g}_{x,y}(t) \rangle = \frac{16}{N^2 C_0^2 \left(\sum_i^R \left[\frac{f^i K_D^i}{(C_0 + K_D^i)^2} \right] \right)^2} \langle Z_{1,2}(s) Z_{1,2}(t) \rangle. \quad (\text{D4})$$

The correlation functions for Z_1 can be written in terms of the single receptor correlation function in the following way

$$\langle Z_1(s)Z_1(t) \rangle = \left\langle \left(\sum_i^R \left[\sum_n^{N^i} x_n^i(s) \cos(\varphi_n^i) \right] \right) \left(\sum_i^R \left[\sum_n^{N^i} x_n^i(t) \cos(\varphi_n^i) \right] \right) \right\rangle \quad (\text{D5})$$

$$= \left\langle \sum_i^R \sum_j^R \sum_n^{N^i} \sum_m^{N^j} x_n^i(s) \cos(\varphi_n^i) x_m^j(t) \cos(\varphi_m^j) \right\rangle \quad (\text{D6})$$

$$= \sum_i^R \sum_j^R \sum_n^{N^i} \sum_m^{N^j} \langle x_n^i(s) x_m^j(t) \rangle \cos(\varphi_n^i) \cos(\varphi_m^j). \quad (\text{D7})$$

Eukaryotic cells are often reaction-limited [28]. In this case, it is appropriate to think of receptors as having simple on-off kinetics, with the rate of binding to a receptor of type i exposed to concentration C is $k_+^i C$ and the off rate is k_-^i – which results in an exponential single receptor correlation function

$$\langle x_n^i(s) x_n^i(t) \rangle = \sigma_{x_n^i}^2 e^{-|t-s|/\tau_n^i} + \langle x_n^i \rangle^2 \quad (\text{D8})$$

for receptor n of type i . The parameter $\sigma_{x_n^i}^2$ characterizes the fluctuations in the occupancy of the receptor, and is given by

$$\sigma_{x_n^i}^2 = \frac{C_n^i K_D^i}{(C_n^i + K_D^i)^2}, \quad (\text{D9})$$

the variance of a Bernoulli trial. τ_n^i is the single receptor correlation time

$$\tau_n^i = 1/(k_-^i + C_n^i k_+^i) \quad (\text{D10})$$

in the reaction-limited case. (Generalization to other limits is possible but not straightforward [29–31].) Because different receptors are independent, the mean of their product is just the product of their means

$$\langle x_n^i(s) x_m^j(t) \rangle = \langle x_n^i(s) \rangle \langle x_m^j(t) \rangle \quad \text{if } i \neq j \text{ or } n \neq m. \quad (\text{D11})$$

Using Eq. D8 for terms where $i = j$ and $n = m$ and Eq. D11 otherwise, we can expand the correlation function of Z_1 in Eq. D7 as

$$\langle Z_1(s)Z_1(t) \rangle = \sum_i^R \sum_j^R \sum_n^{N^i} \sum_m^{N^j} \langle x_n^i(s) x_m^j(t) \rangle \cos(\varphi_n^i) \cos(\varphi_m^j) \quad (\text{D12})$$

$$= \sum_i^R \sum_n^{N^i} \sigma_{x_n^i}^2 e^{-|t-s|/\tau_n^i} \cos^2(\varphi_n^i) + \sum_i^R \sum_j^R \sum_n^{N^i} \sum_m^{N^j} \langle x_n^i(s) \rangle \langle x_m^j(t) \rangle \cos(\varphi_n^i) \cos(\varphi_m^j). \quad (\text{D13})$$

The second term in Eq. D13 is $\langle Z_1 \rangle^2$, which can be solved as

$$\langle Z_1 \rangle^2 = \frac{1}{16} N^2 C_0^2 \left(\sum_i^R \left[\frac{f^i K_D^i}{(C_0 + K_D^i)^2} \right] \right)^2 g_x^2. \quad (\text{D14})$$

by Eq. C16. For the first term in Eq. D13, taking the sum to an integral gives

$$\sum_i^R \sum_n^{N^i} \sigma_{x_n^i}^2 e^{-|t-s|/\tau_n^i} \cos^2(\varphi_n^i) = \frac{N C_0}{2} \sum_i^R f^i \frac{K_D^i}{(C_0 + K_D^i)^2} e^{-|t-s|/\tau^i} + O(g^2), \quad (\text{D15})$$

where $\tau^i = 1/(k_-^i + C_0 k_+^i)$, ie, Eq. D10 for a receptor in the ambient concentration C_0 . Therefore, for shallow gradients, the correlation function for Z_1 is

$$\langle Z_1(s)Z_1(t) \rangle = \frac{N C_0}{2} \sum_i^R f^i \frac{K_D^i}{(C_0 + K_D^i)^2} e^{-|t-s|/\tau^i} + \frac{1}{16} N^2 C_0^2 \left(\sum_i^R \left[\frac{f^i K_D^i}{(C_0 + K_D^i)^2} \right] \right)^2 g_x^2. \quad (\text{D16})$$

Using the relation in Eq. D4, the correlation function of the estimator \hat{g}_1 can be found from Eq. D16:

$$\langle \hat{g}_1(s)\hat{g}_1(t) \rangle = \frac{8 \sum_i^R \left[\frac{f^i K_D^i}{(C_0 + K_D^i)^2} e^{-|t-s|/\tau^i} \right]}{N C_0 \left(\sum_i^R \frac{f^i K_D^i}{(C_0 + K_D^i)^2} \right)^2} + g_x^2. \quad (\text{D17})$$

Similar expressions for the correlation functions of Z_2 and \hat{g}_2 can be derived as

$$\langle Z_2(s)Z_2(t) \rangle = \frac{N C_0}{2} \sum_i^R f^i \frac{K_D^i}{(C_0 + K_D^i)^2} e^{-|t-s|/\tau^i} + \frac{1}{16} N^2 C_0^2 \left(\sum_i^R \left[\frac{f^i K_D^i}{(C_0 + K_D^i)^2} \right] \right)^2 g_y^2 \quad (\text{D18})$$

and

$$\langle \hat{g}_2(s)\hat{g}_2(t) \rangle = \frac{8 \sum_i^R \left[\frac{f^i K_D^i}{(C_0 + K_D^i)^2} e^{-|t-s|/\tau^i} \right]}{N C_0 \left(\sum_i^R \frac{f^i K_D^i}{(C_0 + K_D^i)^2} \right)^2} + g_y^2. \quad (\text{D19})$$

Thus, the correlation in $\hat{\mathbf{g}}$ for shallow gradients is

$$\langle \hat{\mathbf{g}}(s) \cdot \hat{\mathbf{g}}(t) \rangle = \frac{16 \sum_i^R \left[\frac{f^i K_D^i}{(C_0 + K_D^i)^2} e^{-|t-s|/\tau^i} \right]}{N C_0 \left(\sum_i^R \frac{f^i K_D^i}{(C_0 + K_D^i)^2} \right)^2} + g^2. \quad (\text{D20})$$

This now gives us enough information to compute the time-averaged variance,

$$\sigma_{g,T}^2 = \frac{1}{T^2} \int_0^T dt \int_0^T ds \left(\langle \hat{\mathbf{g}}(s)\hat{\mathbf{g}}(t) \rangle - \langle \hat{\mathbf{g}} \rangle^2 \right). \quad (\text{D21})$$

Then, using the result in Eq. D20, we have

$$\sigma_{g,T}^2 = \frac{16 \sum_i^R \left[\frac{f^i K_D^i}{(C_0 + K_D^i)^2} \int_0^T dt \int_0^T ds e^{-|t-s|/\tau^i} \right]}{T^2 N C_0 \left(\sum_i^R \frac{f^i K_D^i}{(C_0 + K_D^i)^2} \right)^2} \quad (\text{D22})$$

$$= 2 \sigma_{\mathbf{g}}^2 \frac{\sum_i^R \frac{f^i K_D^i}{(C_0 + K_D^i)^2} \tau^i \left[T - \tau^i \left(1 - e^{-T/\tau^i} \right) \right]}{T^2 \sum_i^R \frac{f^i K_D^i}{(C_0 + K_D^i)^2}}. \quad (\text{D23})$$

In the limit where $T \gg \tau^i$ for all τ^i , Eq. D23 becomes

$$\sigma_{g,T}^2 = 2 \sigma_{\mathbf{g}}^2 \frac{\sum_i^R \frac{f^i K_D^i}{(C_0 + K_D^i)^2} \tau^i}{T \sum_i^R \frac{f^i K_D^i}{(C_0 + K_D^i)^2}} = \frac{32 \sum_i^R f^i \beta^i \tau^i}{N T \left(\sum_i^R f^i \beta^i \right)^2}, \quad (\text{D24})$$

where the parameter $\beta^i = C_0 K_D^i / (C_0 + K_D^i)^2$ reflects the accuracy of measuring only using receptor i , as in the main text.

Appendix E: Maximum likelihood using full binding trajectory

Instead of simply performing a naive average, a cell could also improve its sensing of the gradient by determining an estimate of the gradient from the history of its receptors over the measurement time – when they are bound and unbound (Fig. 6). We a time interval for receptor n of type i as time series $\{t_{+,n}^i, t_{-,n}^i\}$, where particles bind at times $t_{+,n,\ell}^i$ and unbind at times $t_{-,n,\ell}^i$, where ℓ indexes the binding and unbinding events. Following [20], we compute the probability for a time series of binding and unbinding events. Define a function

$$f_{-,n}^{*,i}(t_{-,n,\ell}^i) = p_{-,n,\ell}^i(t_{-,n,\ell}^i | t_{+,1;n}^i, t_{-,1;n}^i, \dots, t_{-,n-1;n}^i, t_{+,n,\ell}^i) \quad (\text{E1})$$

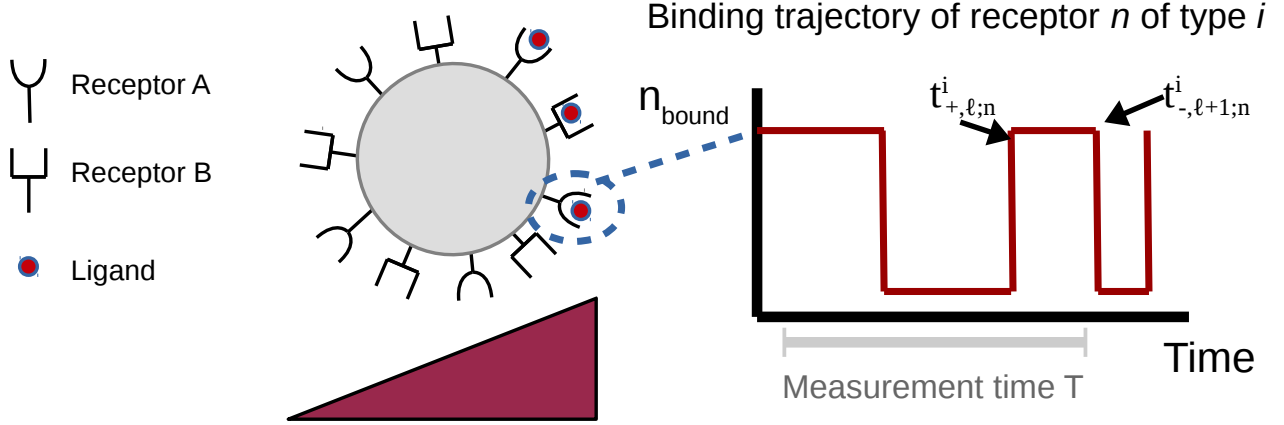


FIG. 6: Illustration of data used for maximum likelihood estimate from full receptor trajectories

which is the probability density for the event that receptor n of type i experiences an unbinding at time $t_{-, \ell; n}^i$ given the previous time series data $\{t_{+, 1; n}^i, t_{-, 1; n}^i, \dots, t_{-, \ell-1; n}^i, t_{+, \ell; n}^i\}$. Define the analogous function

$$f_{+, n}^{*, i}(t_{+, \ell; n}^i) = p_{+, \ell; n}^i(t_{+, \ell; n}^i | t_{-, 1; n}^i, t_{+, 1; n}^i, \dots, t_{+, \ell-1; n}^i, t_{-, \ell-1; n}^i) \quad (E2)$$

for binding events. Then, the probability of observing a time series $\{t_{+, n}^i, t_{-, n}^i\}$ is given by

$$p(\{t_{+, n}^i, t_{-, n}^i\}) = \prod_{\ell}^{\eta_n^i} f_{-, n}^{*, i}(t_{-, \ell; n}^i) f_{+, n}^{*, i}(t_{+, \ell; n}^i) \quad (E3)$$

where $\eta_{b; n}^i, \eta_{u; n}^i$ are the numbers of binding events and unbinding events, respectively. If a cell measures for a time interval T that is long compared to the relevant time scales (ie, $T \gg 1/k_-^i, T \gg 1/C_0 k_+^i$ for all receptor types), then $\eta_{b; n}^i \approx \eta_{u; n}^i$ because the number of binding events can differ by at most one from the number of unbinding events. In this limit, the information about the gradient is dominated by the observed time series, and not the initial snapshot state of the receptors.

We assume that we are in the reaction-limited case, where we can treat the rate of binding to a receptor of type i exposed to concentration C as $k_+^i C$ and the off rate as k_-^i – neglecting rebinding. This limit, as discussed in more detail by [20], is also the appropriate one to find the fundamental bound to accuracy. The functions $f_{-, n}^{*, i}(t_{-, \ell; n}^i)$ and $f_{+, n}^{*, i}(t_{+, \ell; n}^i)$, with this simple Markovian kinetics, do not depend on the whole time series, they only depend on the time of previous unbinding/binding event:

$$f_{-, n}^{*, i}(t_{-, \ell; n}^i) = k_-^i e^{-k_-^i (t_{-, \ell; n}^i - t_{+, \ell-1; n}^i)} \quad (E4)$$

$$f_{+, n}^{*, i}(t_{+, \ell; n}^i) = k_+^i C_n^i e^{-k_+^i C_n^i (t_{+, \ell; n}^i - t_{-, \ell; n}^i)}. \quad (E5)$$

These are probability density functions for exponential distributions with rates k_-^i and $k_+^i C_n^i$ for unbinding and binding, respectively. From these equations, we can determine the likelihood function for the gradient parameters g_x and g_y given the observed time series $\{t_{+, n}^i, t_{-, n}^i\}$ at receptors n of types i . Because each receptor is independent, the likelihood function is the product of the probability function in Eq. E3:

$$\mathcal{L} = \prod_i^R \prod_n^{N^i} \left(\prod_{\ell}^{\eta_{b; n}^i} \left[k_-^i e^{-k_-^i (t_{-, \ell; n}^i - t_{+, \ell-1; n}^i)} \right] \prod_{\ell}^{\eta_{u; n}^i} \left[k_+^i C_n^i e^{-k_+^i C_n^i (t_{+, \ell; n}^i - t_{-, \ell; n}^i)} \right] \right). \quad (E6)$$

Then, define the total time bound $\mathcal{T}_{b;n}^i$ and the total time unbound $\mathcal{T}_{u;n}^i$ for receptor n of type i

$$\mathcal{T}_{b;n}^i = \sum_{\ell}^{\eta_{b;n}^i} t_{-,\ell;n}^i - t_{+,\ell-1;n}^i \quad (\text{E7})$$

$$\mathcal{T}_{u;n}^i = \sum_{\ell}^{\eta_{u;n}^i} t_{+,\ell;n}^i - t_{-,\ell;n}^i. \quad (\text{E8})$$

With these definitions, the likelihood function in Eq. E6 becomes

$$\mathcal{L} = \prod_i^R \prod_n^{N^i} (k_-^i)^{\eta_{b;n}^i} (k_+^i C_n^i)^{\eta_{u;n}^i} e^{-k_-^i \mathcal{T}_{b;n}^i} e^{-k_+^i C_n^i \mathcal{T}_{u;n}^i}. \quad (\text{E9})$$

The log-likelihood function is then

$$\ln \mathcal{L} = \sum_i^R \sum_n^{N^i} \eta_{b;n}^i \ln (k_-^i) + \eta_{u;n}^i \ln (k_+^i C_n^i) - k_-^i \mathcal{T}_{b;n}^i - k_+^i C_n^i \mathcal{T}_{u;n}^i. \quad (\text{E10})$$

Substitution the expression $C_n^i = C_0 \exp \left[\frac{1}{2} (g_x \cos(\phi_n^i) + g_y \sin(\phi_n^i)) \right]$ in Eq. E10 gives

$$\begin{aligned} \ln \mathcal{L} = & \sum_i^R \sum_n^{N^i} \left\{ \eta_{b;n}^i \ln (k_-^i) + \eta_{u;n}^i \ln (k_+^i C_0) + \eta_{u;n}^i \left[\frac{1}{2} (g_x \cos(\phi_n^i) + g_y \sin(\phi_n^i)) \right] - \right. \\ & \left. k_-^i \mathcal{T}_{b;n}^i - k_+^i C_0 \exp \left[\frac{1}{2} (g_x \cos(\phi_n^i) + g_y \sin(\phi_n^i)) \right] \mathcal{T}_{u;n}^i \right\}. \end{aligned} \quad (\text{E11})$$

For shallow gradients, we can approximate the log-likelihood function by expanding to second order in the magnitude of the gradient. This results in

$$\begin{aligned} \ln \mathcal{L} \approx & \sum_i^R \sum_n^{N^i} \left\{ \eta_{b;n}^i \ln (k_-^i) + \eta_{u;n}^i \ln (k_+^i C_0) + \eta_{u;n}^i \left[\frac{1}{2} (g_x \cos(\phi_n^i) + g_y \sin(\phi_n^i)) \right] - k_-^i \mathcal{T}_{b;n}^i \right. \\ & \left. - k_+^i C_0 \left[1 + \frac{1}{2} (g_x \cos(\phi_n^i) + g_y \sin(\phi_n^i)) + \frac{1}{8} (g_x \cos(\phi_n^i) + g_y \sin(\phi_n^i))^2 \right] \mathcal{T}_{u;n}^i \right\}. \end{aligned} \quad (\text{E12})$$

Differentiating Eq. E12 with respect to g_x and g_y , we get

$$\frac{\partial}{\partial g_x} \ln \mathcal{L} = \sum_i^R \sum_n^{N^i} \left\{ \frac{\eta_{u;n}^i}{2} \cos(\phi_n^i) - k_+^i C_0 \left[\frac{1}{2} \cos(\phi_n^i) + \frac{1}{4} (g_x \cos(\phi_n^i) + g_y \sin(\phi_n^i)) \cos(\phi_n^i) \right] \mathcal{T}_{u;n}^i \right\} \quad (\text{E13})$$

$$\frac{\partial}{\partial g_y} \ln \mathcal{L} = \sum_i^R \sum_n^{N^i} \left\{ \frac{\eta_{u;n}^i}{2} \sin(\phi_n^i) - k_+^i C_0 \left[\frac{1}{2} \sin(\phi_n^i) + \frac{1}{4} (g_x \cos(\phi_n^i) + g_y \sin(\phi_n^i)) \sin(\phi_n^i) \right] \mathcal{T}_{u;n}^i \right\}. \quad (\text{E14})$$

Because g_x and g_y here do not depend on i and n , Eq. E14 can be equated to zero and solved to find the maximum likelihood estimator in terms of sums over functions of $\mathcal{T}_{u;n}^i$ and ϕ_n^i . However, we have not found the precise form very useful. From the derivatives of the log-likelihood function, we can compute the Fisher Information Matrix:

$$\mathcal{I}_{a,b} = - \left\langle \frac{\partial^2}{\partial a \partial b} \ln \mathcal{L} \right\rangle. \quad (\text{E15})$$

Differentiating Eq. E13 and Eq. E14 gives the following matrix

$$\mathcal{I} = \begin{bmatrix} \sum_i^R \sum_n^{N^i} \frac{k_+^i C_0 \langle \mathcal{T}_{u;n}^i \rangle}{4} \cos^2(\phi_n^i) & \sum_i^R \sum_n^{N^i} \frac{k_+^i C_0 \langle \mathcal{T}_{u;n}^i \rangle}{4} \cos(\phi_n^i) \sin(\phi_n^i) \\ \sum_i^R \sum_n^{N^i} \frac{k_+^i C_0 \langle \mathcal{T}_{u;n}^i \rangle}{4} \cos(\phi_n^i) \sin(\phi_n^i) & \sum_i^R \sum_n^{N^i} \frac{k_+^i C_0 \langle \mathcal{T}_{u;n}^i \rangle}{4} \sin^2(\phi_n^i) \end{bmatrix}. \quad (\text{E16})$$

The expectation value $\langle \mathcal{T}_{u;n}^i \rangle$ can be found in terms of the measurement time T and the probability P_n^i that a receptor is occupied (Eq. C2)

$$\langle \mathcal{T}_{u;n}^i \rangle = T(1 - P_n^i) = T \frac{K_d^i}{C_n^i + K_d^i}. \quad (\text{E17})$$

By substituting Eq. E17 into Eq. E16 and taking the inner sums to an integral, we have the following expressions for each matrix element:

$$\begin{aligned} \sum_i^R \sum_n^{N^i} \frac{k_+^i C_0 \langle \mathcal{T}_{u;n}^i \rangle}{4} \cos^2(\phi_n^i) &= \frac{1}{4} \sum_i^R \frac{N^i}{2\pi} \int_0^{2\pi} \frac{k_+^i C_0 T K_d^i}{(C_0 \exp[\frac{g}{2} \cos(\varphi - \phi)] + K_d^i)} \cos^2(\phi) d\phi \\ &= N \sum_i^R \frac{f^i k_-^i C_0 T}{8(C_0 + K_d^i)} + O(g^2) \end{aligned} \quad (\text{E18})$$

$$\begin{aligned} \sum_i^R \sum_n^{N^i} \frac{k_+^i C_0 \langle \mathcal{T}_{u;n}^i \rangle}{4} \sin^2(\phi_n^i) &= \frac{1}{4} \sum_i^R \frac{N^i}{2\pi} \int_0^{2\pi} \frac{k_+^i C_0 T K_d^i}{(C_0 \exp[\frac{g}{2} \cos(\varphi - \phi)] + K_d^i)} \sin^2(\phi) d\phi \\ &= N \sum_i^R \frac{f^i k_-^i C_0 T}{8(C_0 + K_d^i)} + O(g^2) \end{aligned} \quad (\text{E19})$$

$$\sum_i^R \sum_n^{N^i} \frac{k_+^i C_0 \langle \mathcal{T}_{u;n}^i \rangle}{4} \cos(\phi_n^i) \sin(\phi_n^i) = \frac{1}{4} \sum_i^R \frac{N^i}{2\pi} \int_0^{2\pi} \frac{k_+^i C_0 T K_d^i}{(C_0 \exp[\frac{g}{2} \cos(\varphi - \phi)] + K_d^i)} \cos(\phi_n^i) \sin(\phi_n^i) d\phi = 0. \quad (\text{E20})$$

Therefore, the Fisher information matrix is diagonal, and in shallow gradients it is

$$\mathcal{I} = \begin{bmatrix} NC_0 T \sum_i^R \frac{f^i k_-^i}{8(C_0 + K_d^i)} & 0 \\ 0 & NC_0 T \sum_i^R \frac{f^i k_-^i}{8(C_0 + K_d^i)} \end{bmatrix}. \quad (\text{E21})$$

We note that this is the large- T limit; in the limit of $T \rightarrow 0$, we would expect the Fisher information to limit to the estimate from a single snapshot.

For cells with a single receptor, Eq. E21 implies that the asymptotic variances on g_x and g_y are 1/2 of their value determined from time averaging—the same factor as in concentration sensing [20]. However, in the multiple receptor limit, there is a more significant difference. The variance in $\hat{\mathbf{g}}$ determined from Eq. E21 is the sum of the inverses of the diagonal elements

$$\sigma_{g,T;MLE}^2 = \frac{16}{NC_0 T \sum_i^R \frac{f^i k_-^i}{(C_0 + K_d^i)}} = \frac{16}{NC_0 \sum_i^R \frac{f^i K_d^i}{(C_0 + K_d^i)^2} \frac{T}{\tau^i}}. \quad (\text{E22})$$

Appendix F: Extended data on hedging

Within the main paper, we have presented the optimal configuration of receptors as a function of the environment. However, at large environmental uncertainties, the benefit from hedging bets may not be as large. We show extended data corresponding to Fig. 1 and Fig. 4 in the main paper in Fig. 7 and Fig. 8.

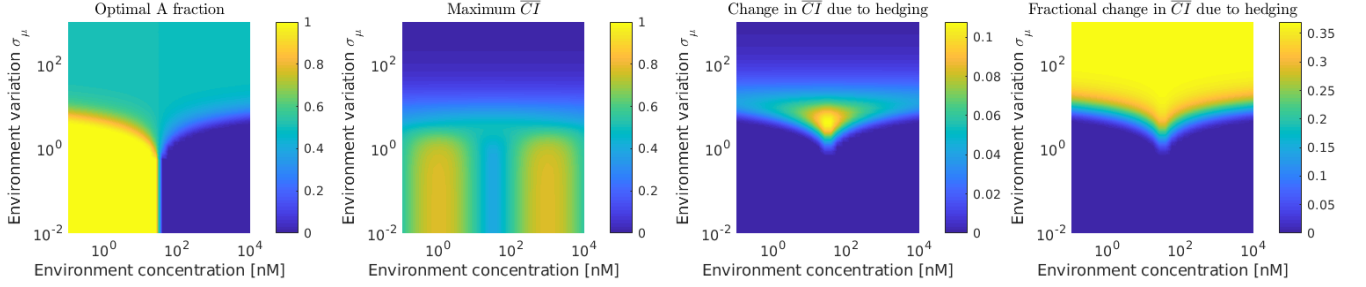


FIG. 7: Tradeoffs in snapshot sensing. This figure complements Fig. 1 in the main text, showing how, with the same parameters, the maximum \overline{CI} depends on the uncertainty (2nd panel). The third and fourth panel show the increase in the mean CI due to hedging, i.e. the change vs all- A or all- B (whichever of these is better). The largest absolute improvements in \overline{CI} due to hedging are at intermediate uncertainties; in the limit of truly high uncertainties, no configuration creates a large \overline{CI} .

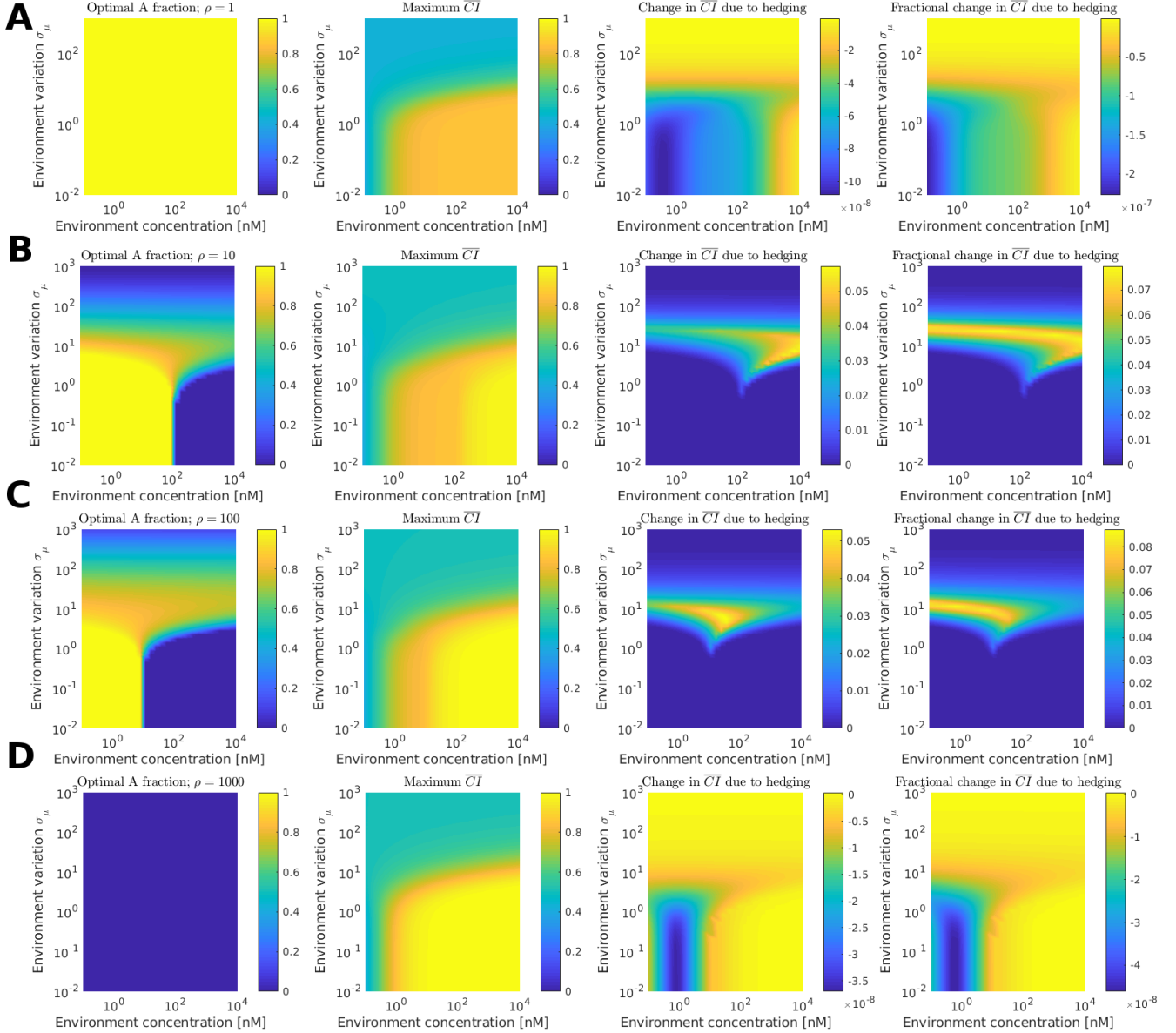


FIG. 8: Tradeoffs in time-averaged sensing. This figure shows the maximum \overline{CI} and increase in \overline{CI} due to hedging for the time-average case. This corresponds to Fig. 4 in the main paper, with the left panels redrawing that data. We show the values for A) $\rho = 1$, B), $\rho = 10$, C) $\rho = 100$, D) $\rho = 1000$. Note that for A) and D), the change in mean CI due to hedging is slightly negative – the optimal configuration is all- A or all- B , but our optimization does not recover $f_A = 0, 1$ with numerical precision.